

## Heat transfer studies in natural carbonates from San Juan (Argentina)

H.S. Silva\*, J.W. Romero, R.B. Venturini, J.E. González

*Instituto de Ingeniería Química, Departamento de Física, Facultad de Ingeniería, Universidad Nacional de San Juan,  
Av. Libertador San Martín 1109 (Oeste), Dpto. Capital (5400) San Juan, Argentina*

Received 14 June 2000; accepted 15 June 2000

### Abstract

A method based on the analysis of the temperature profiles is proposed to identify changes in the physical structure and/or in the chemical composition of a solid when a constant heat flow passes through it. This analysis is applied to natural carbonates which are important from an industrial point of view. The thermal conductivity of the calcined and non-calcined natural carbonates is determined in order to relate variations in the temperature profiles with changes in the structure of the solids under study. A mathematical model, which predicts temperature profiles in spherical samples for heat transport processes similar to those studied, is proposed. This model is able to predict temperature profiles in heat transport processes, with or without chemical reaction, and with the chemical reaction fitting the progressive conversion model or the unreacted core one. © 2000 Elsevier Science B.V. All rights reserved.

*Keywords:* Natural carbonates; Heat transfer; Thermal decomposition; Temperature profile; Mathematical model

### 1. Introduction

Natural carbonates are minerals widely spread in the earth crust. Some of these minerals are considered as important calcium and magnesium sources for different purposes. In San Juan (Argentina), naturally occurring calcium and/or magnesium carbonates are limestone, travertine and dolostone. Geological reserves of limestone in San Juan (e.g. Villicum, Retamito, Jáchal), account for more than 5000 million tons, and reserves of travertine (e.g. La Laja, El Salado) reach to 150 million tons. Limestone production in Argentina is about 10 million tons per year and travertine production is 35,000 t per year [1]. According to their geological origin, dolostones from several deposits in San Juan (e.g. Villicum, Sierra Chica de

Zonda, Retamito) have different magnesium contents. Primary and secondary dolostones, which were recognised by macroscopic and stratigraphical analysis, have been reported [2]. Dolostone production in Argentina is about 6000 t per year and geological reserves account for more than 400 million tons [3].

One of the main industrial processes, in which these natural carbonates are utilised is their thermal decomposition to obtain calcium and magnesium oxides. Thus, studies aiming to obtain information for the design of new production units or to optimise the existing ones are very important.

For design purposes, a mathematical model which describes reactant and product flows along the reactor has to be adopted, and mass and energy balances have to be solved [4]. This procedure requires the knowledge of parameters that characterise the heat and mass transport processes between solid and gas phases. Those are the convective and radiative heat transport

\* Corresponding author. Fax: +54-264-4200289.  
E-mail address: hsilva@unsj.edu.ar (H.S. Silva).

coefficient, the coefficient for heat transport in the solid phase (i.e. thermal conductivity of calcined and non-calcined mineral), the coefficient for mass transport in the solid phase (i.e. effective diffusion) and the coefficient for mass transport in the boundary layer between solid and fluid phases [5]. It is also necessary to know the chemical reaction kinetics, which includes the global reaction order and the reaction rate constant and its dependence with temperature [6–8]. The above mentioned coefficients have to be evaluated, either to validate mathematical models [9–11] reported as suitable for similar reaction systems [12–14], or to propose new ones.

In order to study the thermal decomposition of dolostones, another aspect has to be considered. Some of them behave as mechanical mixtures of calcium carbonate and magnesium carbonate, and others as ‘double salt’, in which calcium and magnesium ions are distributed in a unique crystalline structure [15]. Dolostones from San Juan-Argentina, belong to the latter type, as reported in kinetic studies [16].

From a theoretical point of view, selective calcination processes are feasible in dolostones of the ‘mechanical mixture’ type. In dolostones of the ‘double salt’ type, a selective thermal decomposition is not feasible. In this case, as in limestone and travertine calcination, the main reactor design problem is to determine the time necessary to reach a given conversion.

Limestone, dolostone and travertine from San Juan-Argentina, have been studied. All tested samples have shown surface areas between 5 and 10 m<sup>2</sup>/g. A limestone from Neuquén-Argentina, which has different geological genesis and physical properties (i.e. surface area and porosity) is also studied to investigate the influence of these properties on the behaviour of these carbonates under thermal decomposition.

One of the goals of this investigation is the determination of the thermal conductivity of calcined and non-calcined natural carbonates. For spherical samples submitted to thermal decomposition, a method based on the analysis of the temperature profile is proposed. This method allows to decide which mathematical model, unreacted core or progressive conversion, adjusts the thermal decomposition of these minerals. Furthermore, a mathematical model, which predicts temperature profiles similar to those observed in spherical samples under thermal decomposition, is proposed.

## 2. Experimental

### 2.1. Thermal conductivity measurement

The experimental arrangement used to measure the thermal conductivities is shown in Fig. 1. Basically, the energy supplied by an electric heater flows axially through cylindrical samples of the carbonate under study (0.1 m diameter and 0.025 m height). The radial heat flow is minimised placing a heat-insulating layer around the lateral surface of the samples. The temperature of the high and low temperature surfaces is sensed with K-type (chromel–alumel) thermocouples inserted in each base of both samples ( $T_{c1}$ ,  $T_{c2}$ ,  $T_{c3}$  and  $T_{c4}$ ). Those temperatures are set regulating the power supply (high temperature surface) and using a thermostatic bath (low temperature source).

The heat transmitted from the high temperature surface to the low temperature one is dissipated in two heat-exchange units. This is accomplished by means of a cooling liquid proceeding from the thermostatic bath. The energy is supplied to the system through a VARITRANS transformer (220 V input voltage, 0–250 V output voltage) and is measured with a NORMA wattmeter (electromagnetic instrument, class 0.2, range in AC, 0.5–1 A, range in AV, 75–600 V, test voltage 2 KV).

The temperatures of the hot and cold surfaces are measured with a digital HANSEN multimeter (range in DC, 200  $\mu$ A–10 A, range in DCV 200 MV–1000 V, range in ACV, 200–750 V). A GOSSEN multimeter (range in AC, 60 mA–6 A, range in ACV, 6–600 V) is used to protect the wattmeter. A COLORA thermostatic bath (mod. NB36130, 50–1500 W heating resistances, 273–373 K temperature control range and circulating pump) was used as cold source. Energy is supplied to the heater regulating the output voltage of the transformer, in order to set the temperature of the hot surface ( $T_{hot}$ ) at about 303 K. The thermostatic bath temperature ( $T_{cold}$ ), is regulated 5 K below the hot surface temperature. In this way, it is possible to determine thermal conductivities and their variations with temperature, in case they occur.

When the thermal equilibrium is achieved, temperatures of the thermocouples  $T_{c1}$ ,  $T_{c2}$ ,  $T_{c3}$  and  $T_{c4}$  are measured. This procedure is repeated for higher temperatures, keeping the differences between  $T_{hot}$

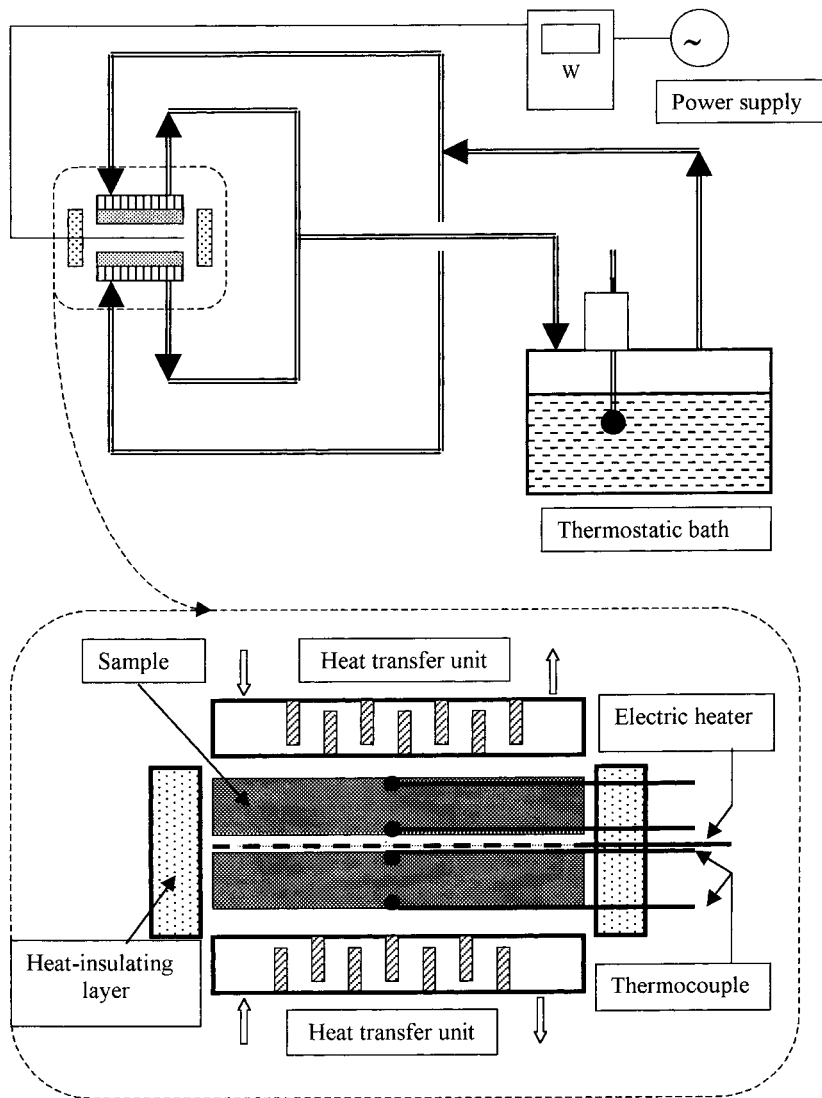


Fig. 1. Experimental arrangement for thermal conductivity measurement.

and  $T_{\text{cold}}$  almost constant, until the low temperature source reaches  $\approx 353$  K.

The thermal conductivity of the material is calculated by Eq. (1)

$$k = \frac{(e_1 + e_2)P}{4A\Delta T} \quad (1)$$

$(e_1 + e_2)$  is the total length of the cylindrical samples (m),  $P$  the power supplied to the solid through an electric resistance (W),  $A$  the area of the hot and cold

surfaces ( $\text{m}^2$ ),  $k$  the thermal conductivity of the solid ( $\text{W/m K}$ ),  $\Delta T$  the temperature difference between the hot and cold surfaces (K).

The results of an experimental test are summarised in Tables 1–6. This procedure is used to determine thermal conductivities of calcined and non-calcined carbonates studied. Three experimental tests were carried out for both, non-calcined and calcined minerals, and thermal conductivities for these materials were determined (Tables 2–6).

Table 1  
Experimental results from a typical test to determine the thermal conductivity of non-calcined dolostone

No.	$T_{\text{cold}}$ (K)	$T_{\text{hot}}$ (K)	$\Delta T$ (K)	$P$ (W)	$k$ (W/m K)	$T_{\text{prom}}$ (K)
1	312.5	319	6.5	13	3.186	315.75
2	321.5	330	8.5	19	3.558	325.75
3	322	331	9	19	3.360	326.5
4	324	333	9	18.5	3.267	328.5
5	329.5	339.5	10	19	3.023	334.5
6	331.5	340.5	9	19	3.360	336.0
7	337	349.5	12.5	27	3.442	343.25
8	338.5	351.5	13	27	3.308	345.0
9	343.5	356.5	13	27.5	3.360	350.0
10	345.5	358.5	13	27	3.308	352.0
11	348.5	362	13.5	27.5	3.244	355.25

Table 2  
Experimental results from a typical test to determine the thermal conductivity of calcined dolostone

No.	$T_{\text{cold}}$ (K)	$T_{\text{hot}}$ (K)	$\Delta T$ (K)	$P$ (W)	$k$ (W/m K)	$T_{\text{prom}}$ (K)
1	308	313	5.0	3.6	1.146	310.5
2	312	317	5.0	3.8	1.210	314.5
3	318	325	7.0	4.5	1.024	321.5
4	322	329.5	7.5	5.5	1.167	325.75
5	326	333	7.0	5.5	1.251	329.5
6	331	339	8.0	5.5	1.094	335.0
7	338	347	9.0	7.0	1.238	343.5
8	343	353	10.0	7.5	1.195	348.0
9	347.5	357.5	10.0	7.5	1.195	352.5
10	351	362.5	11.5	8.0	1.107	356.75

## 2.2. Temperature profiles study

An spherical sample of each rock studied is used to carry out the temperature profile analysis. The samples

are spherical in order to obtain a good isometric energy transfer. These conditions are attained by means of a previous determination of the temperature profile of the furnace. The isometric heat transfer

Table 3  
Experimental results from a typical test to determine the thermal conductivity of non-calcined travertine

No.	$T_{\text{cold}}$ (K)	$T_{\text{hot}}$ (K)	$\Delta T$ (K)	$P$ (W)	$k$ (W/m K)	$T_{\text{prom}}$ (K)
1	310	314	4	7.1	2.826	312
2	314	319	5	8.2	2.61	316.5
3	318	323	5	8.7	2.77	320.5
4	324	329.5	5.5	10.0	2.90	326.75
5	328	335	7	11.3	2.57	331.5
6	332	338.5	6.5	11.3	2.768	335.25
7	338	345	7	11.5	2.616	341.5
8	344	351	7	12.0	2.73	347.5
9	351.5	359.5	8	14.2	2.826	355.5
10	355	365	10	16.5	2.677	360
11	359.5	369.5	10	18.2	2.90	364.5

Table 4  
Experimental results from a typical test to determine the thermal conductivity of calcined travertine

No.	$T_{\text{cold}}$ (K)	$T_{\text{hot}}$ (K)	$\Delta T$ (K)	$P$ (W)	$k$ (W/m K)	$T_{\text{prom}}$ (K)
1	310	315	5	3.2	1.019	312.5
2	314.5	320.5	6	4.2	1.114	317.5
3	319	326	7	4.5	1.023	322.5
4	323	330.5	7.5	4.6	0.976	326.75
5	328.5	336	7.5	5.8	1.23	332.25
6	334	342.5	8.5	5.8	1.086	338.25
7	338	348	10	5.8	0.923	343.0
8	342	352.5	10.5	6.3	0.955	347.25
9	347	357	10	6.5	1.035	352.0
10	350	361	11	7.8	1.129	357.5

Table 5  
Experimental results from a typical test to determine the thermal conductivity of non-calcined limestone

No.	$T_{\text{cold}}$ (K)	$T_{\text{hot}}$ (K)	$\Delta T$ (K)	$P$ (W)	$k$ (W/m K)	$T_{\text{prom}}$ (K)
1	310	314	4	8.75	3.483	312
2	318	323	5	12	3.821	320.5
3	325	330.5	5.5	13.5	3.908	327.25
4	334.5	340.5	6	14.5	3.848	337.5
5	338	344.5	6.5	15.5	3.8	341.25
6	342.5	349.5	7	17.5	3.98	346
7	347	354.5	7.5	17.0	3.715	350.75
8	350	358	8	17.5	3.483	354
9	354	362	8	18.0	3.58	356
10	358	367	9	19.5	3.45	360.5

conditions are ensured placing the spherical sample in a position in which five thermocouples, located at the same depth in the solid, measure the same temperature.

To obtain the temperature profile, four thermocouples,  $T_{s_0}$ ,  $T_{s_1}$ ,  $T_{s_2}$  and  $T_{s_3}$  are placed at different

depths ( $R_0=0.035$ ,  $R_1=0.025$ ,  $R_2=0.015$  and  $R_3=0.005$  m) in a spherical sample ( $R_0=0.035$  m) of non-calcined carbonate. The temperature of the gas surrounding the sample is measured by thermocouple  $T_{s_5}$ . The temperature difference between the muffle furnace and the sample surface is controlled by an

Table 6  
Experimental results from a typical test to determine the thermal conductivity of calcined limestone

No.	$T_{\text{cold}}$ (K)	$T_{\text{hot}}$ (K)	$\Delta T$ (K)	$P$ (W)	$k$ (W/m K)	$T_{\text{prom}}$ (K)
1	312	317	5	5.5	1.75	314.5
2	315	322	7	6	1.365	318.5
3	320	325.5	5.5	6	1.737	322.75
4	323.5	330	6.5	7	1.715	326.75
5	327	335.5	8.5	8	1.5	331.25
6	331	339.5	8.5	8.5	1.592	335.25
7	335	342.5	7.5	8.5	1.8	338.75
8	340	349.5	9.5	9	1.508	344.75
9	344	354	10	10	1.592	349
10	349	360	11	12.5	1.809	354.5

interactive control software based on PC which allows for the simultaneous measurement of eight thermocouples.

At temperatures below 623 K, the exchange of heat between the gas surrounding the sample and the solid surface takes place mainly by convection, because radiation and conduction are negligible at these temperatures. Then, in this case, the differential rate of heat flow is:

$$dQ = h_c(T_g - T_0)dA_s \quad (2)$$

$dQ$  is the differential rate of heat flow,  $h_c$  the heat transfer coefficient by convection,  $T_g$  the temperature of the gas surrounding the sample,  $T_0$  the temperature of the solid surface and  $dA_s$  the differential area of the solid.

If the experiment is carried out under isometric energy transfer conditions,  $T_g - T_0$  is constant for all points of the solid surface, then, in this case, the rate of heat flow is:

$$Q = 4\pi h_c R_0^2 (T_g - T_0) \quad (3)$$

If the temperature profile analysis is carried out keeping  $(T_g - T_0)$  constant, according to Eq. (3)  $Q$  is constant. In the range of temperatures above mentioned, and under isometric heat transfer conditions, no changes in the physical structure and in the chemical composition of the materials are expected. Therefore, the temperature gradient across a shell limited by two spherical surfaces (radii  $R_i$  and  $R_{i+1}$ ), may be calculated by Eq. (4) [9,17].

$$Q = \frac{4\pi R_i R_{i+1} k (T_i - T_{i+1})}{R_i - R_{i+1}} \quad (4)$$

$k$  is the thermal conductivity of the solid and  $(T_i - T_{i+1})$  the temperature gradient across the shell.

When the decomposition temperature of the solids studied is reached (i.e. above 900 K), the heat transfer between the gas and the solid surface takes place mainly by radiation, because conduction and convection are negligible at these temperatures. Then, the rate of heat flow is given by:

$$Q = 4\pi h_r R_0^2 (T_g^4 - T_0^4) \quad (5)$$

where  $h_r$  is the heat transfer coefficient by radiation. The temperature control system is programmed to keep  $(T_g^4 - T_0^4)$  constant.

### 3. Results and discussion

#### 3.1. Thermal conductivity calculation

Applying Eq. (1), thermal conductivities of natural carbonates from San Juan-Argentina are determined. No variation of thermal conductivities with temperature over the range tested are found. The values obtained are:

Thermal conductivity of non-calcined dolostone:

$$k_{ncd} = 3.17 \pm 0.04$$

Thermal conductivity of calcined dolostone:

$$k_{cd} = 1.14 \pm 0.01$$

Thermal conductivity of non-calcined limestone:

$$k_{ncl} = 3.75 \pm 0.02$$

Thermal conductivity of calcined limestone:

$$k_{cl} = 1.61 \pm 0.01$$

Thermal conductivity of non-calcined travertine:

$$k_{nct} = 2.75 \pm 0.02$$

Thermal conductivity of calcined travertine:

$$k_{ct} = 1.08 \pm 0.01$$

#### 3.2. Temperature profile analysis

(a) At constant heat flow regime, and when the sample temperature is lower than the thermal decomposition temperature of all tested materials (carbonates from San Juan and Neuquén), temperature profiles show similar characteristics (Curve A of Fig. 2).

The temperature gradient across every shell adjust to Eq. (4). Temperature profiles show that heat flows from the gas surrounding the solid to the interior of the sample. Different temperature gradients are observed in equivalent shells of every tested materials. This is due to their different thermal conductivities.

(b) When the thermal decomposition temperature of each carbonate is reached, substantial variations in the temperature profiles corresponding to limestone, dolostone and travertine from San Juan, are observed in comparison with that of Curve A of Fig. 2. These are due to the beginning of the chemical reaction.

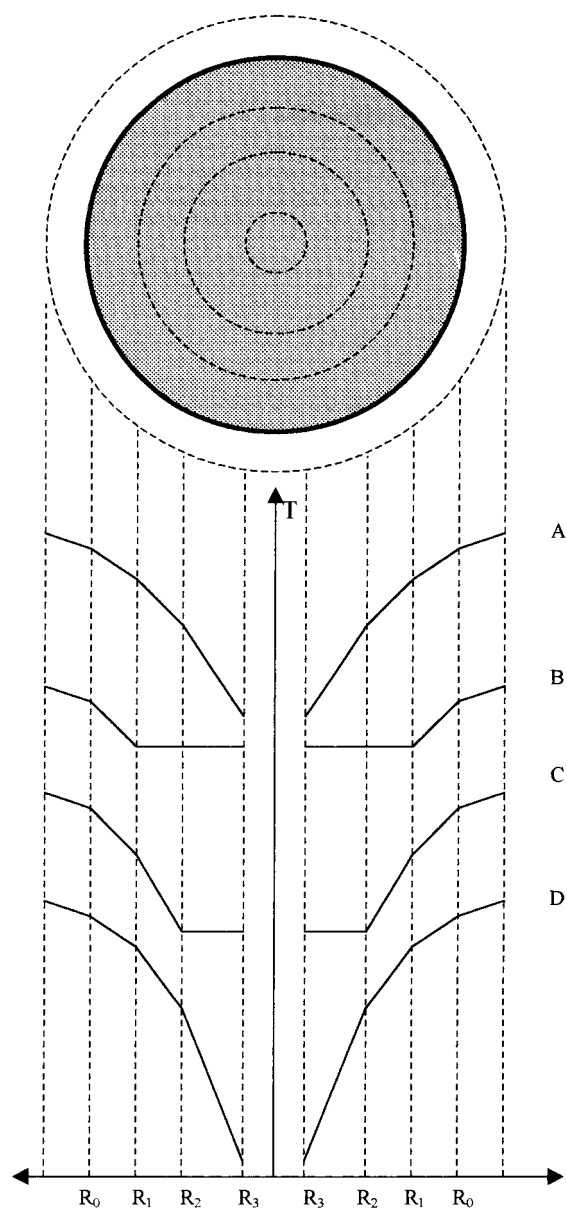


Fig. 2. Temperature profiles in spherical samples: (A) before calcination, (B) and (C) under calcination, (D) after calcination.

The whole analysis for these carbonates can be summarised as follows:

(b.1) Below the temperature at which the chemical reaction occurs at a reasonable rate, the temperature profile keeps the shape of curve A in Fig. 3.

(b.2) From this point on, the temperatures of thermocouples  $T_{S_1}$ ,  $T_{S_2}$  and  $T_{S_3}$  tend to equalise and the temperature profile shown by curve B on Fig. 2, is obtained. The whole energy that reaches the solid surface is totally consumed by the chemical reaction that takes place in the outer shell (the one limited by two spherical surfaces, radii  $R_0$  and  $R_1$ ). Heat does not reach the inner part of the solid and the core temperature tends to homogenise.

(b.3) The outer shell has already reacted and the heat passes through the newly formed material (the corresponding oxides) and the thermal decomposition of the material between thermocouples  $T_{S_1}$  and  $T_{S_2}$  begins.

During this period, the temperatures of thermocouples  $T_{S_2}$  and  $T_{S_3}$  tend to equalise. The observed temperature profile corresponds to curve C in Fig. 2. This means that the heat that reaches the solid passes through the shell limited by thermocouples  $T_{S_0}$  and  $T_{S_1}$ , and is totally consumed by the chemical reaction in the shell limited by thermocouples  $T_{S_1}$  and  $T_{S_2}$ .

(b.4) When the sample is totally converted, the temperature profile shows temperature gradients in all shells, (curve D in Fig. 2). This behaviour agrees with that of heat transport processes in totally calcined carbonate species. The above mentioned conclusions show that thermal decomposition of limestone, dolostone and travertine from San Juan is a chemical reaction that fits the unreacted core model, in which the mass transfer process is the control step. This is because, although the whole sample reached the decomposition temperature, the carbon dioxide formed in the chemical reaction diffuses through the calcined carbonate, which has high porosity, but not through the non-calcined carbonate, which shows a negligible one.

(c) The temperature profile observed during the thermal decomposition of limestone from Neuquén is similar to that obtained before the beginning of the chemical reaction (Curve A in Fig. 2), because the thermal decomposition takes place in the whole volume of the sample. In this case, temperature gradients change with time in every shell, due to the progressive conversion of carbonates into oxides. Carbon dioxide diffuses through calcined and non-calcined material. Thus, the thermal decomposition of this material fits the progressive conversion model.

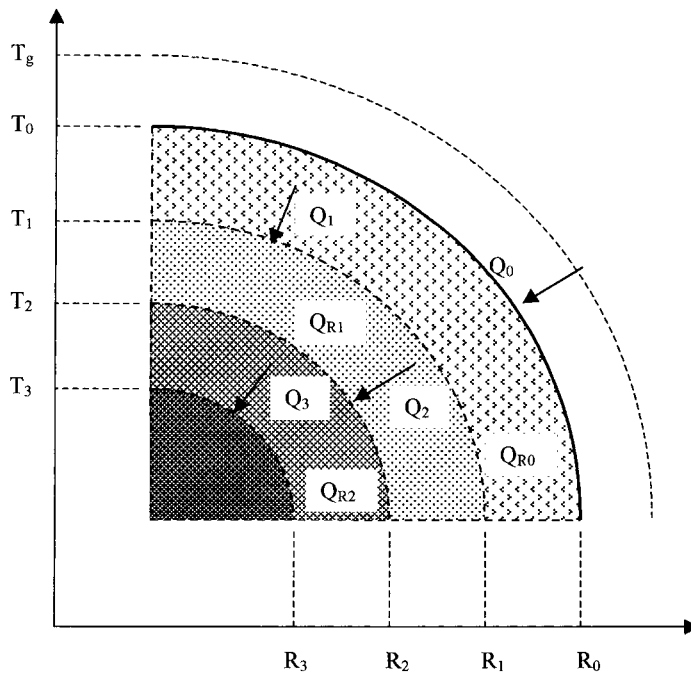


Fig. 3. Heat flow through concentric shells: # 1 (limited by thermocouples placed at  $R_0$  and  $R_1$ ), # 2 (limited by thermocouples placed at  $R_1$  and  $R_2$ ) and #3 (limited by thermocouples placed at  $R_2$  and  $R_3$ ) when  $Q_0$  passes through the surface of a spherical sample.

### 3.3. Mathematical model for the thermal decomposition of carbonates

A mathematical model is proposed to explain the temperature profile observed in the thermal decomposition of natural carbonates studied. Basically, a heat balance over consecutive concentric shells of the spherical sample, is carried out. From this analysis, the temperature gradients across each shell are determined.

#### Heat balance over shell # 1 (between $R_0$ and $R_1$ )

The heat that passes through the solid surface of the sample ( $Q_0$ ) is equal to the energy used to carry out the chemical reaction ( $Q_{R_0}$ ) plus the energy entering the next shell ( $Q_1$ ) (Fig. 3).

$$Q_0 = 4\pi h_c R_0^2 (T_g - T_0) \quad (6)$$

$$Q_1 = \frac{R_1 R_0 k (T_0 - T_1)}{R_0 - R_1} \quad (7)$$

$$Q_{R_0} = \frac{4}{3} \pi (\Delta H_r) (r_{Q_0}) (R_0^3 - R_1^3) \quad (8)$$

where  $Q_0$  is the heat flow from the gas to the surface of the solid,  $Q_{R_0}$  the heat consumed by the chemical

reaction at  $T_0$ ,  $Q_1$  the heat flow through the spherical surface of radius  $R_1$ ,  $h_c$  the heat transfer coefficient of the boundary layer,  $T_g$  the gas temperature,  $T_0$  the temperature of the solid surface,  $R_0$  the sample radius,  $R_1$  the spherical surface radius at which thermocouple  $T_{s_1}$  is placed,  $T_1$  the thermocouple  $T_{s_1}$  temperature,  $\Delta H_r$  the heat of reaction,  $r_{Q_0}$  the chemical reaction rate at  $T_0$ ,  $k$  the thermal conductivity of the solid.

$$4\pi h_c R_0^2 (T_g - T_0) = \frac{R_1 R_0 k (T_{s_0} - T_{s_1})}{R_0 - R_1} + \frac{4}{3} \pi (\Delta H_r) (r_{Q_0}) (R_0^3 - R_1^3) \quad (9)$$

$$T_1 = T_0 - \frac{(Q_0 - Q_{R_0})(R_0 - R_1)}{k R_0 R_1} \quad (10)$$

From the heat balance over shell #2 (between  $R_1$  and  $R_2$ )

$$T_2 = T_1 - \frac{(Q_1 - Q_{R_1})(R_1 - R_2)}{k R_1 R_2} \quad (11)$$

$Q_{R_1}$  is the heat consumed by the chemical reaction at  $T_{s_1}$ ,  $T_2$  the thermocouple  $T_{s_2}$  temperature.



From the heat balance over shell # 3

$$T_3 = T_2 - \frac{(Q_2 - Q_{R_2})(R_2 - R_3)}{kR_2R_3} \quad (12)$$

$Q_{R_1}$  is the heat consumed by the chemical reaction at  $T_2$ ,  $Q_2$  the heat flow through the spherical surface of radius  $R_2$  and  $T_3$  the thermocouple  $T_{s_3}$  temperature.

Three cases are analysed using Eqs. (10)–(12). The first one corresponds to the heat flow through the whole sample volume, in which no chemical reaction is occurring (Curve A in Fig. 2). In this case  $Q_{R_0} = Q_{R_1} = Q_{R_2} = 0$ , and Eqs. (10)–(12), become Eq. (4).

The second case corresponds to the chemical reaction adjusting the unreacted core model. Then,

$$Q_1 = Q_2 = Q_{R_1} = Q_{R_2} = 0$$

for the chemical reaction occurring in the first shell. This makes

$$T_1 = T_2 = T_3$$

as shown in curve B of Fig. 3.

When the chemical reaction is taking place in the shell # 2, the heat flow passes through shell # 1 ( $Q_{R_0} = 0$ ) and  $T_1$  is obtained from Eq. (12).

In addition

$$Q_2 = Q_{R_2} = 0$$

Then,

$$T_2 = T_3$$

This is observed in curve C of Fig. 3.

The third case corresponds to the chemical reaction adjusting the progressive conversion model. Eqs. (10)–(12) predict temperature gradients across all shells as the thermal decomposition of the mineral occurs. This is because

$$Q_0 \neq Q_{R_0}, \quad Q_1 \neq Q_{R_1}$$

and

$$Q_2 \neq Q_{R_2}$$

This is observed in the thermal decomposition of limestone from Neuquén, which has higher porosity and surface area than natural carbonates from San Juan.

## 4. Conclusions

Changes in the physical structure and/or in the chemical composition of a solid material can be identified by means of the temperature analysis reported here. To recognise those changes, the thermal conductivity of the solid must be known because the temperature gradients observed are related to the material through which heat flows.

The proposed mathematical model can also be used to predict the temperature profile of heat transport processes, with or without chemical reaction and with chemical reaction adjusting to the progressive conversion model or to the unreacted core one.

The proposed method could also be applied to other gas–solid systems, only if the thermal conductivity of the reactants is different from that of the reaction products.

## Acknowledgements

The authors wish to thank Dr. L.M. Petkovic for her helpful comments and suggestions in writing this paper.

## References

- [1] Unified System of Mining Information. Secretaría de Industria Comercio y Minería de la Nación (Argentina), (1999) (<http://www.suim.gov.ar/alfanum/>).
- [2] O. Bordonaro, A. Arroqui, Potencial de Magnesio de las Dolomitas Cámbricas de San Juan, Argentina, V Congreso Nacional de Geología Económica, San Juan, Argentina, 1996, pp. 215–221.
- [3] E. Dublanc, D. Malca, A. Pérez, Industrial minerals of Argentina — Looking for investment, *Industrial Minerals Buenos Aires (Argentina)* 312 (1993) 25.
- [4] H.S. Silva, D.L. Granados, Dimensionamiento de un Reactor de Lecho Móvil para la Descomposición Térmica de Dolomitas, *Información Tecnológica, La Serena, (Chile)* 9 (2) (1998) 125–130.
- [5] B.D. Kulkarni, L.K. Doraiswamy, Estimation of effective transport properties in packed bed reactors, *Cat. Rev. Sci. Eng., New York* 22 (3) (1980) 431–483.
- [6] A.E. Mericboyu, S. Kükükbayrac, Kinetic analysis of non isothermal calcination TG curves of natural Turkish dolomites, *Thermochimica Acta, Amsterdam* 232 (1994) 225–232.
- [7] H.S. Silva, J.W. Romero, N.D. Martínez, C. Acosta, Cinética de Calcinación de Dolomitas — Una Ecuación Basada en las

- Condiciones de Operación, Información Tecnológica, La Serena, (Chile) 10 (4) (1999) 137–142.
- [8] A.E. Mericboyu, S. Kükükbayrac, B. Dürüs, Evaluation of the kinetic parameters for the thermal decomposition of natural Turkish limestones from their thermogravimetric curves using a computer programme, *J. Thermal Anal. London* 39 (1993) 707–714.
- [9] G. Narsimhan, Thermal decomposition of calcium carbonate, *Chem. Eng. Sci. London* 16 (1961) 7–20.
- [10] S. Ulkutan, T. Dogu, S. Dogu, Structural variations as a tool to analyze the mechanism of non catalytic solid–gas reactions, *Chem. Reaction Eng., Washington* 40 (1982) 515–525.
- [11] M. Ishida, C.Y. Wen, Comparison of kinetic and diffusional models for solid–gas reactions, *J. Am. Chem. Soc., Washington* 14 (2) (1968) 311–317.
- [12] L.K. Doraiswamy, M.M. Sharma, *Heterogeneous Reactions: Analysis, Examples and Reactor Design*, Wiley, New York, 1984, 468 pp (Chapter 19).
- [13] J.J. Carberry, *Ingeniería de las Reacciones Químicas y Catalíticas*, McGraw-Hill, New York, 1980, 358 pp (Chapter 7).
- [14] L.H. Farina, O.A. Ferreti, G.F. Barreto, *Introducción al Diseño de Reactores Químicos*. Eudeba. 1° Ed., Buenos Aires, 1986, 776 pp (Chapter 15).
- [15] R.E. Kirk, D.F. Othmer, *Encyclopedia of Chemical Technology*, Wiley, New York 8, 1981, 609 pp.
- [16] J.C. Pedregosa, J.W. Romero, H.S. Silva, M.C. Viola *Análisis Termodinámico y Cinético de la Descomposición Térmica de Dolomitas*. X Congreso Argentino de Fisicoquímica. Tucumán, Argentina, 1997.
- [17] R.H. Perry, D.W. Green, *Perry's Chemical Engineerings Handbook*, McGraw-Hill, 6th Edition, New York, 1984, pp. 4–10 (Chapter 10).